Synthesis and characterization of novel mesoporous aluminosilicate MCM-41 containing aluminophosphate building units

Tomás D. Conesa,[a] Robert Mokaya,[a] Juan M. Campelo[b] and Antonio A. Romero*[b]

Received (in Cambridge, UK) 8th December 2005, Accepted 15th March 2006
First published as an Advance Article on the web 3rd April 2006
DOI: 10.1039/b517450c

Novel MCM-41 aluminosilicate/aluminophosphate materials that exhibit good mesostructural ordering have been synthesized and characterised; the synthesis of these silicoaluminophosphates involved the use of gel mixtures containing amorphous mesoporous aluminosilicate and aluminophosphate phases as precursor.

Research on the synthesis and development of aluminium containing mesoporous molecular sieves is important due to the potential application of such materials as catalysts and catalyst supports. However, the amorphous pore walls, weak acidity and low hydrothermal stability of mesoporous aluminosilicates limit their use as catalysts.[1,2] On the other hand, aluminophosphate (AlPO) and silicoaluminophosphate (SAPO) molecular sieves are known to exist in a wide range of structural and compositional diversity. The most studied group of AlPO and SAPO materials are microporous in nature. However, microporous AlPO and SAPO materials cannot be used as catalysts for reactions involving bulky molecules because of their small pores. Larger pore mesoporous AlPO materials have been synthesized by several groups.[3–7] Moreover, relatively thermally stable metal-substituted mesoporous AlPO materials containing Ti, Co, Mg, Fe, Zr and V have also been reported.[8–14]

The incorporation of Si in AlPO molecular sieves generates acidity and results in materials that are active for acid catalysed reactions. However, only a few studies dealing with the substitution of Si in the framework of mesoporous AlPOs have been reported.[15–18] Here, we report a new approach for the synthesis of mesoporous SAPO materials with high Si loading *via* the addition of aluminophosphate precursors to preformed mesoporous aluminosilicate MCM-41 phases. We have studied the influence of aluminophosphate content on the mesostructural ordering, textural properties, surface acidity and catalytic activity of the resulting SAPO materials.

A two step procedure was used to prepare the SAPO materials at $[SiO_2 + Al_2O_3]/AlPO_4$ molar ratios between 2 and 6. The samples were designated as SiAlP-X, where X = 6, 4.5, 3 or 2 is the molar ratio in the synthesis gel. Step 1 involved the preparation of the MCM-41 aluminosilicate precursor (gel A) and aluminophosphate precursor (gel B). A typical synthesis procedure (sample SiAlP-4.5) was as follows. The MCM-41 aluminosilicate precursor phase (Si/Al = 30) was prepared by mixing 20 g of cetyltrimethylammonium bromide (CTAB) with 100 ml of H_2O, followed by addition of 0.44 g of aluminium triisopropoxide, 200 ml of ethanol (96% v/v) and 200 ml of ammonia (25% NH_3). The mixture was homogenized for 10 min, and then 14.4 ml of tetraethyl orthosilicate (TEOS) was slowly added. After stirring for 1 h at room temperature the aluminosilicate gel was obtained. The aluminophosphate precursor (P/Al = 1) was prepared by mixing 1.9 g of CTAB, 3 g of aluminium triisopropoxide and 35 ml of H_2O. After stirring for 10 min, 1 ml of H_3PO_4 (85 wt% solution in water) was added drop by drop. The mixture was stirred at room temperature for 1 h, resulting in the aluminophosphate precursor gel. In step 2, gel B was added to gel A under vigorous stirring to obtain the final silicoaluminophosphate synthesis gel. The resulting gel was homogenized for 1 h, and then transferred into an autoclave and hydrothermally treated at 373 K for 24 h. The solids thus obtained were separated by filtration and dried in air overnight at 293 K. The washing step was avoided because it diminished the mesostructural ordering of the final solids. The dry samples were calcined in air by heating to 873 K at 10 K/min and then maintaining at 873 K for 12 h.

Samples were characterized by XRD (Siemens D-5000 diffractometer with CuKα), N_2 sorption (Micromeritics ASAP 2000 sorptometer), and ^{29}Si, ^{27}Al and ^{31}P MAS NMR (ACP-400 multinuclear spectrometer) analysis. Surface acidity was measured using pyridine (Py) as the probe molecule,[19] and catalytic activity was evaluated for the continuous flow vapour-phase Beckmann rearrangement of cyclohexanone oxime into ε-caprolactam at 723 K.

Table 1 shows the molar composition of the final gel mixtures (expressed as Si, Al, P oxide mol %) and the composition of calcined SiAlP samples (obtained by Inductively Coupled Plasma, IRIS Intrepid Instrument, Thermo Electron Corporation). The compositional data reveal that phosphorus was not completely incorporated into the solid for samples synthesized at 373 K.

Table 1 Composition of the final synthesis gel mixture and the SiAlP-X solid products

	Final gel mixture			Calcined samples		
Sample	SiO_2	Al_2O_3	P_2O_5	SiO_2	Al_2O_3	P_2O_5
SiAlP-6	83.8	8.5	7.7	84.5	11.2	4.3
SiAlP-4.5	80.6	10.5	8.9	81.9	12.7	5.4
SiAlP-3	73.8	13.7	12.5	76.9	16.7	6.4
SiAlP-3(423)[a]	73.8	13.7	12.5	80.9	10.4	8.7
SiAlP-2	65.7	17.8	16.5	69.9	21.5	8.7

[a] Synthesised *via* hydrothermal treatment at 423 K.

---

[a] *School of Chemistry, University of Nottingham, University Park, Nottingham, UK NG7 2RD. E-mail: r.mokaya@nottingham.ac.uk; Fax: +44 115 9513562; Tel: +44 115 8466174*
[b] *Departamento de Química Orgánica, Universidad de Córdoba, Campus de Rabanales, Edificio Marie Curie (C-3), Ctra. N-IV Km., 396 14014-Córdoba, Spain. E-mail: qo1rorea@uco.es; Fax: +34 957212066; Tel: +34 957218638*

However, in the SiAlP-3(423) sample, synthesized at 423 K, the incorporation of phosphorus into the calcined solid improved.

Fig. 1 shows the low-angle powder XRD patterns of calcined SiAlP samples. Three peaks are observed for SiAlP-6 and SiAlP-4.5 samples, indicating a highly ordered pore channel system with long-range order. The peaks are indexed to (100), (110) and (200) diffractions of a hexagonal mesoporous MCM-41 type lattice. As the $AlPO_4$ content increased, the mesostructural ordering of the samples deteriorated as indicated by broadening and decrease in intensity of the XRD peaks. We attribute these changes to either partial loss of long-range structural ordering or formation of Al_2O_3 and/or $AlPO_4$ species within the mesopores. No XRD peaks were observed in the high angle region (5–80°) thus confirming that there were no other ordered phases apart from the MCM-41 mesostructure.

The nitrogen sorption isotherms of the SiAlP samples are shown in Fig. 2A. All the calcined samples exhibit type IV isotherms, typical of mesoporous solids. The isotherms of samples SiAlP-6 and SiAlP-4.5 exhibit a well-defined step between $P/P_0 = 0.2$ and 0.35, characteristic of capillary condensation within mesopores. The sharpness of this step suggests a uniform pore size system (as shown in Fig. 2B) and provides evidence of the high quality of these samples. The increase in nitrogen uptake at high pressure ($P/P_0 > 0.9$) is indicative of a significant amount of interparticle mesoporosity. The textural properties of the samples are summarised in Table 2. The decrease in surface area, pore volume and pore size as the $AlPO_4$ content increased (Table 2) is attributed to the formation of Al_2O_3 and/or $AlPO_4$ species within the mesopores, which may partially block the pores of the mesostructure. Hence, the incorporation of a great amount of aluminophosphate precursor disrupted the quality of the final SiAlP silicoaluminophosphate mesoporous materials, in agreement with XRD results (Fig. 1).

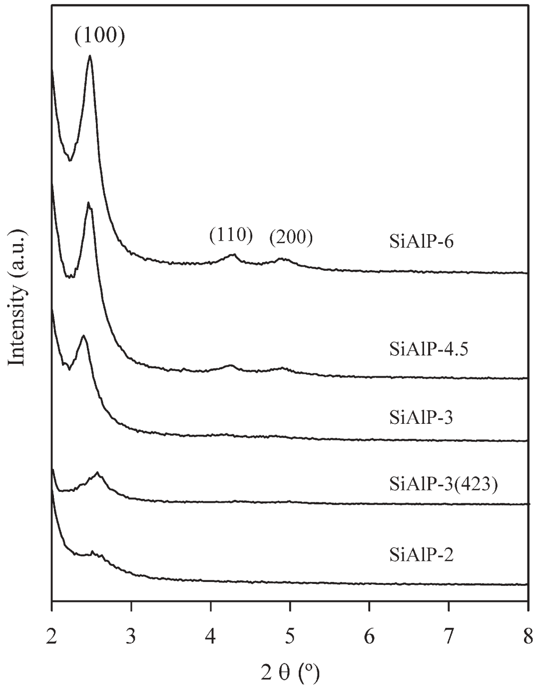

Fig. 1 Powder XRD patterns of calcined SiAlP-X materials.

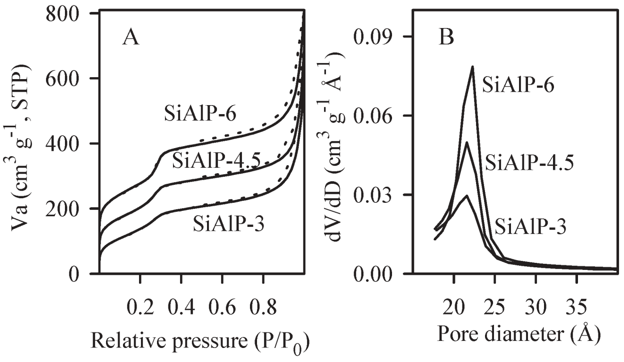

Fig. 2 (A) Nitrogen sorption isotherms and (B) pore size distribution (PSD) curves of calcined SiAlP-X materials. PSD curves were obtained *via* BJH analysis of adsorption data.

Table 2 Textural properties and acidity of calcined SiAlP-X samples

Sample	a_o[a] (Å)	Surface area ($m^2 g^{-1}$)	Pore volume ($cm^3 g^{-1}$)	Pore size[b] (Å)	WT[c] (Å)	Acidity (μmol g^{-1})
Al-MCM-41[d]	42	1047	0.91	23 (3)	19	116
SiAlP-6	41	692	0.55	22 (3)	19	93
SiAlP-4.5	41	603	0.53	21 (4)	20	93
SiAlP-3	41	516	0.51	20 (5)	21	85
SiAlP-3(423)	43	401	0.39	20 (6)	23	45
SiAlP-2	38	321	0.29	18 (7)	21	77

[a] The lattice parameter a_o is obtained by the formula $a_o = 2d_{100}/\sqrt{3}$, where d_{100} is basal spacing from XRD patterns. [b] Pore size obtained from BJH analysis of nitrogen adsorption data (values in parentheses are the width at half-height (Å) of PSD curve). [c] WT is wall thickness, calculated as WT = a_o − pore size. [d] (Si/Al = 30), included for comparative purposes.

The acidity of the samples (reported as amount, μmol/g, of pyridine adsorbed at 573 K)[19] is given in Table 2. We observed higher total acidity for the SiAlP samples compared to that of amorphous AlPO mesoporous materials previously reported by Campelo *et al.*[20] However, the total acidity was lower than that of aluminosilicate MCM-41, and decreased at higher $AlPO_4$ content (Table 2). As noted above, the surface area also decreased at higher $AlPO_4$ content; therefore, the acid density [(μmol of Py adsorbed/g of catalyst)/(m^2 of surface area/g of catalyst)] was higher for our SiAlP silicoaluminophosphate materials compared to both Al-MCM-41 and amorphous mesoporous AlPO[20] materials. The higher density of acid sites is expected to translate to higher catalytic activity for the SiAlP materials.

The local environment of Si, Al and P atoms in the calcined SiAlP samples was studied by MAS NMR analysis. The peaks in the ^{29}Si MAS NMR spectra (not shown) were very broad and similar to those obtained for amorphous silica and M41S materials.[19] The ^{27}Al MAS NMR spectra of the hydrated calcined SiAlP samples (Fig. 3; SiAlP-4.5 as an example) were similar to those previously reported for mesoporous AlPOs[4,9] and mesoporous SAPOs.[8,9,17] There were two peaks in the ^{27}Al MAS NMR spectra of our SAPO samples at *ca.* 37 ppm and −2.5 ppm. The peak at 37 ppm was assigned to tetrahedrally coordinated Al bonded to phosphorus atoms *via* oxygen bridges.[4,9,17,20] The peak at −2.5 ppm was attributed to octahedrally coordinated Al.[4,9,17] The broad peak width of both resonances for the SiAlP materials

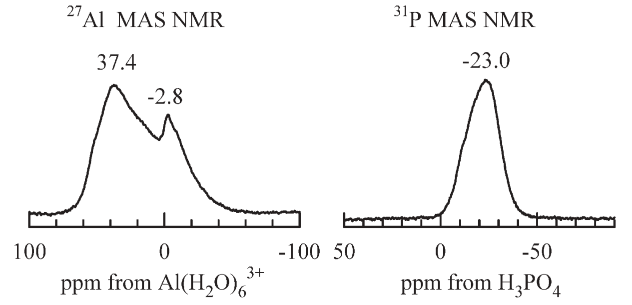

Fig. 3 ^{27}Al and ^{31}P MAS NMR spectra of calcined SiAlP-4.5 sample.

Table 3 Product distribution (S_i, mol %) in vapor-phase Beckmann rearrangement of cyclohexanone oxime and durability (*D*, catalyst lifetime at 100 mol % conversion level) on SiAlP catalysts

	Time on stream/24 h						
Catalyst[a]	X_t	$S_{\varepsilon\text{-C}}$	$S_{\text{C-AN}}$	$S_{\text{C-EN}}$	S_{CN}	S_{AN}	*D*/h
Al-MCM-41	100	73.8	12.5	6.5	2.5	4.7	35
SiAlP-6	100	71.6	4.8	9.6	8.1	5.9	29
SiAlP-6[b]	100	64.7	10.4	5.7	8.1	7.7	25
SiAlP-4.5	100	80.7	5.2	5.5	5.1	3.5	31
SiAlP-4.5[b]	92.3	74.4	10.4	6.3	5.9	3.0	19
SiAlP-3	100	83.7	4.2	5.9	3.2	3.0	30
SiAlP-2	100	88.4	3.4	4.1	0.0	4.1	26

[a] Reaction condition: *W*/*F* = 92.8 g h/mol; 0.3 M C-ox in acetonitrile or [b] toluene. X_t is total cyclohexanone oxime conversion.

indicated poor structural ordering of the Al atoms. The ^{31}P MAS NMR spectra of the calcined SiAlP samples (Fig. 3; SiAlP-4.5 as an example) show a broad peak centered *ca.* −23.5 ppm, which is assigned to tetrahedrally coordinated phosphorus.[4,8,9,17,20] The broad peak width indicates a disordered environment of phosphorus atoms in the mesoporous SiAlP samples. However, the ^{31}P MAS NMR data suggested that phosphorus atoms were successfully incorporated into the framework of the SiAlP mesoporous materials.

The results of cyclohexanone oxime (C-ox) conversion, lifetime and selectivity to ε-caprolactam (ε-C), cyclohexanone (C-AN), cyclohexen-1-one (C-EN), cyanopentene (CN) and aniline (AN), at 723 K, on Al-MCM-41 and SiAlP-X catalysts are shown in Table 3. The catalytic data clearly show an increase in selectivity to ε-C as the $[SiO_2 + Al_2O_3]/AlPO_4$ molar ratio decreases. However, durability of the SiAlP samples was lower than that of the Al-MCM-41 catalyst. However, when acetonitrile (highly polar) was used as the solvent, both selectivity to ε-C and durability of the SiAlP catalysts were improved.

In summary, we report a novel route for the preparation of stable mesoporous silicoaluminophosphate molecular sieves with an MCM-41 structure. In contrast to the conventional synthesis strategy for mesoporous SAPO[15–18] in which Si is substituted in the framework of mesoporous AlPO, our synthesis approach involves incorporation of aluminophosphate units into the framework of aluminosilicate MCM-41, resulting in mesoporous SAPO materials with higher silicon loading. We provide strong evidence that the aluminophosphate units were incorporated into the mesoporous aluminosilicate framework. XRD and N_2 sorption studies reveal the partial loss of mesostructural ordering as the aluminophosphate content increased. A high density of acid sites is generated in the SAPO materials, which is reflected in their catalytic activity for the vapour-phase Beckmann rearrangement of cyclohexanone oxime to ε-caprolactam. The catalytic data show that the incorporation of higher amounts of aluminophosphate into Al-MCM-41 promotes selectivity to ε-caprolactam. Our studies show that the potential applications of mesoporous Al-MCM-41 may be widened by incorporating important characteristics found in microporous materials into the mesoporous materials.

This research was subsidized by grants from the Dirección General de Investigación (Project CTQ2005-04080 and CTQ2004-21662-E), Ministerio de Ciencia y Tecnología, FEDER funds, and from the Consejería de Innovación, Ciencia y Empresa (Junta de Andalucía).

Notes and references

1 A. Corma, *Chem. Rev.*, 1997, **97**, 2373.
2 A. Taguchi and F. Schüth, *Microporous Mesoporous Mater.*, 2005, **77**, 1.
3 D. Zhao, Z. Luan and L. Kevan, *Chem. Commun.*, 1997, 1009.
4 T. Kimura, Y. Sugahara and K. Kuroda, *Microporous Mesoporous Mater.*, 1998, **22**, 115.
5 M. Tiemann, M. Schulz, C. Jäger and M. Fröba, *Chem. Mater.*, 2001, **13**, 2885.
6 M. Tiemann and M. Fröba, *Chem. Commun.*, 2002, 406.
7 K. Lin, L. Wang, Z. Sun, Q. Yang, Y. Di, D. Zhang, D. Jiang and F.-S. Xiao, *Chem. Lett.*, 2005, **34**, 516.
8 X. S. Zhao and G. Q. (Max) Lu, *Microporous Mesoporous Mater.*, 2001, **44–45**, 185.
9 Z.-Y. Yuan, T.-H. Chen, J.-Z. Wang and H.-X. Li, *Colloids Surf., A*, 2001, **179**, 253.
10 N. C. Masson and H. O. Pastore, *Microporous Mesoporous Mater.*, 2001, **44–45**, 173.
11 S. K. Mohapatra, B. Sahoo, W. Keune and P. Selvam, *Chem. Commun.*, 2002, 1466.
12 S. K. Mohapatra and P. Selvam, *Chem. Lett.*, 2004, **33**, 198.
13 J.-M. Lü, K. T. Ranjit, P. Rungrojchaipan and L. Kevan, *J. Phys. Chem. B*, 2005, **109**, 9284.
14 Ch. Subrahmanyam, B. Louis, B. Viswanathan, A. Renken and T. K. Varadarajan, *Appl. Catal., A*, 2005, **282**, 67.
15 Y. Z. Khimyak and J. Klinowski, *Phys. Chem. Chem. Phys.*, 2001, **3**, 2544.
16 B. Chakraborty, A. C. Pulikottil, S. Das and B. Viswanathan, *Chem. Commun.*, 1997, 911.
17 X. S. Zhao, G. Q. Lu, A. K. Whittaker, J. Drennan and H. Xu, *Microporous Mesoporous Mater.*, 2002, **55**, 51.
18 B. Rajesh, M. Palanichamy, V. Kazansky and V. Murugesan, *Indian J. Chem., Sect. A*, 2001, **40**, 1262.
19 J. M. Campelo, D. Luna, R. Luque, J. M. Marinas, A. A. Romero, J. J. Calvino and M. P. Rodríguez-Luque, *J. Catal.*, 2005, **230**, 327.
20 J. M. Campelo, M. Jaraba, D. Luna, R. Luque, J. M. Marinas, A. A. Romero, J. A. Navio and M. Macias, *Chem. Mater.*, 2003, **15**, 3352.